ECTI-EEC Transactions Pre-proof

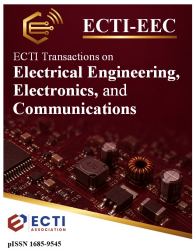

Design of a DC Line Impedance Stabilization Network with an EMI Separator Circuit

Warathep Padungtin, and Vuttipon Tarateeraseth

DOI: http://doi.org/10.37936/ecti-eec.2027251.267900

Reference: ECTI-EEC 267900

Received date: 6 September 2026

Accepted date: 10 November 2026

This is a PDF of an article that has been improved after acceptance, including the inclusion of a cover page and metadata, as well as the optimization of readability. Before its publication in its final form, this version will undergo further copyediting, typesetting, and review. As a result, this version is no longer the Accepted Manuscript, but it is not yet the definitive **Version of Record**. We are providing this early version to provide the article with early visibility.

Published by ECTI Association Thailand

ECTI Transactions on Electrical Engineering, Electronics, and Communications, Vol. 25, No. 1, pp. 78–86, February 2027

https://doi.org/10.37936/ecti-eec.2027251.267900
ISSN(Online): 1685-9545

Design of a DC Line Impedance Stabilization Network with an EMI Separator Circuit

Warathep Padungtin[1] and Vuttipon Tarateeraseth[2]†

Abstract

This paper presents a design method for a DC line impedance stabilization network (LISN) incorporating an EMI separator circuit for measuring conducted electromagnetic interference (EMI). The proposed DC LISN enables the effective separation of positive-to-ground (P-G), negative-to-ground (N-G), common-mode (CM), and differential-mode (DM) noise from low-voltage equipment under test (EUT). The design is validated experimentally, demonstrating that the proposed DC LISN maintains an impedance of 50 Ω ± 20% over the frequency range of 150 kHz to 30 MHz, in compliance with CISPR 25. Furthermore, the effectiveness of the noise separation is confirmed by the strong agreement between the CM and DM noise measurements obtained using the proposed DC LISN and those obtained using a current probe. Finally, the proposed design provides a substantially lower-cost alternative to commercial solutions while maintaining practical EMI diagnostic capability. It may support industrial research and innovation by complementing pre-compliance testing infrastructure for low-voltage DC equipment in academia and industry.

Keywords: Electromagnetic Interference, EMI Separator, Industrial Research, Innovation, Line Impedance Stabilization Network.

I. Introduction

In recent years, the adoption of DC grids has increased significantly, driven in part by policies aimed at improving power distribution efficiency in various countries. DC grids offer potential advantages over conventional AC grids, particularly in terms of overall system losses, cable length limitations, and cost savings [1]. The integration of renewable electricity sources is also motivated by the need to reduce carbon emissions from power generation. This transition is expected to accelerate the adoption of DC grid systems, which can support clean energy integration through established renewable sources, such as wind and solar power. Recent developments have further demonstrated the reliability and safety of DC grid systems. Numerous studies have investigated their applications across a wide range of sectors, including industry, renewable energy systems, electric vehicles, telecommunications, and building infrastructure. However, as DC grid systems become more widespread, interoperability among multiple power electronic systems becomes increasingly important to ensure seamless integration and accommodate voltage step-up and step-down requirements within existing AC grid infrastructure.

Unfortunately, the operation of electronic devices can lead to malfunctions or unintended damage because these devices may generate electromagnetic interference (EMI) in the form of conducted and radiated emissions, potentially affecting nearby electronic devices or their own operation [2]. Despite the advantages of DC grid systems, electromagnetic compatibility (EMC) remains a significant challenge that cannot be overlooked [3]. Furthermore, EMC issues are complicated by the integration of multiple systems, including the interaction between power line communication (PLC) signals and power system operating frequencies, as well as the operation of Flexible AC Transmission Systems (FACTS). These interactions can exacerbate EMI problems in both wired and wireless communication systems. Currently, DC grids rely on conventional EMC standards originally developed for AC systems, including CISPR 32 and CISPR 16 for conducted emissions, UL 1699B and IEC 63027 for arc-fault detection, and EN 50065 for power line communication. Future EMC frameworks may incorporate adaptive emission limits and enhanced immunity criteria to address the specific challenges of DC microgrids more effectively [4]. Therefore, all electronic devices must comply with stringent EMC standards and requirements [5].

According to EMC standards, line impedance stabilization networks (LISNs) are required for conducted and radiated emissions testing.

The primary functions of LISNs are defined in the CISPR

Manuscript received September 6, 2026; revised on October 31, 2026; accepted November 10, 2026.
Recommended for publication by Associate Editor Yuttana Kumsuwan.
†Corresponding Author: Vuttipon Tarateeraseth (vuttipon@g.swu.ac.th)
[1]Turnkey and Infrastructure, ALSTOM Transport Systems, Bangkok, Thailand.
[2]Department of Electrical Engineering, Srinakharinwirot University, Nakhonnayok, Thailand.

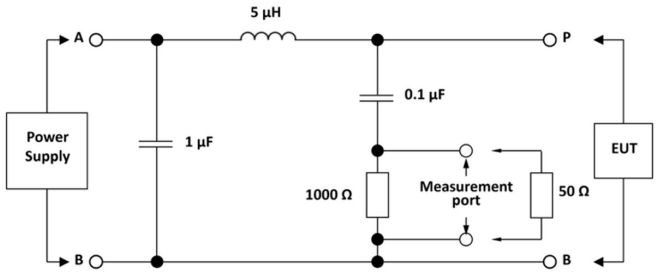

Fig. 1. Equivalent circuit of a LISN based on CISPR 25 for low-voltage equipment.

16-1-2 standard, which specifies that a LISN must maintain the main impedance, either positive-to-ground (P-G) or negative-to-ground (N-G), at 50 Ω ± 20% over the frequency range of 150 kHz to 30 MHz. Additionally, LISNs prevent external EMI from affecting measurement results. However, conducted emissions measured at the P-G and N-G ports of commercial LISNs contain a combination of common-mode (CM) and differential-mode (DM) emissions, making them unsuitable for distinguishing between these noise components during EMI diagnosis. To isolate CM or DM emissions, specialized equipment, such as a current probe [6] or an EMI separator [7], is commonly used. However, these devices can be expensive and may not be readily available for pre-compliance testing.

Therefore, integrating an LISN and an EMI separator into a single measurement device is essential. The development of LISNs and EMI separator circuits has been actively investigated over the years, with LISN design primarily focusing on cost reduction and performance improvement. In [8], a custom-designed LISN compliant with CISPR 16-1-2 is proposed, employing air-core inductors to significantly reduce costs. However, these inductors exhibit a low self-resonant frequency (SRF), which can compromise impedance performance, particularly at high frequencies. To address this limitation, the LISN proposed in [9] employs a toroidal inductor, providing high accuracy at low frequencies. However, unaccounted parasitic elements can lead to impedance instability under certain operating conditions. To overcome the limitations of these inductor-based improvement techniques, a multistage 5-µH LISN is presented in [10] to achieve more stable impedance characteristics. However, the reported schematic exhibits a resonance peak at approximately 1 MHz. Furthermore, an additional device, such as a current probe, is required to distinguish between CM and DM noise. Several techniques for extracting CM and DM noise from measured conducted emissions have been reported in [7, 11–17]. This paper highlights the importance of integrating an LISN and an EMI separator circuit to meet the measurement requirements of DC systems. The proposed DC LISN design method aims to address the limitations of conventional LISN designs, including resonance peaks, the number of measurement ports, and physical constraints. The proposed DC LISN is based primarily on [18] for the LISN component and [14] for the EMI separator circuit. Finally, the performance of the proposed system is experimentally validated to demonstrate compliance with the CISPR 25 standard. The innovation presented in this paper is a unified instrument that integrates a multistage DC LISN with an EMI separator circuit, bridging the gap between separate diagnostic tools. The system supports continuous, simultaneous measurements on both positive and negative power lines without violating CISPR 25 impedance limits. Beyond conceptual integration, this work details the practical PCB realization, embedded protection schemes, and rigorous experimental validation benchmarked against a calibrated current probe. This integrated approach may support industrial research and development by providing a cost-effective component of testing infrastructure for conducted EMI diagnostics and pre-compliance evaluation of low-voltage DC equipment.

This paper is structured as follows: Section II explains the circuit design and provides details on the components used. Section III presents the design methods for the EMI separator circuit. Section IV discusses the validation and analysis of the test results. Finally, Section V summarizes the research findings and highlights the key contributions of this paper.

II. SCHEMATIC DESIGN AND COMPONENT SPECIFICATIONS

This paper proposes an effective DC LISN design for equipment under test (EUTs) particularly in low-voltage (LV) DC systems. A DC-DC converter is selected as the primary EUT because of its low cost and suitability for DC grid applications. The conventional schematic of a 5-μH DC LISN compliant with CISPR 25 is shown in Fig. 1. However, to address the limitations of the conventional DC LISN, a four-stage DC LISN was proposed in [10]. The simulated impedance responses reported in [10] indicate that multistage architectures can exhibit inherent resonance peaks, typically around 1 MHz, due to the self-resonance of the capacitors in each stage. Although these resonances can be mitigated using zero-addition compensation techniques, such approaches often increase the design complexity. Therefore, a modified four-stage DC LISN is adopted in this paper to eliminate the resonance peaks [18]. The topology of the proposed DC LISN has been enhanced beyond that of a conventional DC LISN by incorporating dual-port functionality, enabling continuous EMI noise measurements at both the positive and negative ports. In addition, the proposed DC LISN integrates an EMI separator to simultaneously distinguish between common-mode (CM) and differential-mode (DM) noise. This feature facilitates EMI diagnosis and enables more precise troubleshooting.

The prototype of the proposed DC LISN is designed for DC-powered equipment with a nominal operating voltage range of 0–60 Vdc and a maximum continuous current of 10 A. It has an absolute maximum voltage rating of 200 V and incorporates built-in surge protection. For safety reasons, although the proposed DC LISN is rated for voltages up to 200 V, its operating voltage is limited to 60 Vdc to mitigate the risk of electric shock in the event of an accidental connection between the supply voltage and the housing. The DC LISN operates over a frequency range of 150 kHz to 30 MHz and provides four output ports for simultaneous measurement of positive-to-ground (P-G), negative-to-ground (N-G), common-mode (CM), and differential-mode (DM) noise.

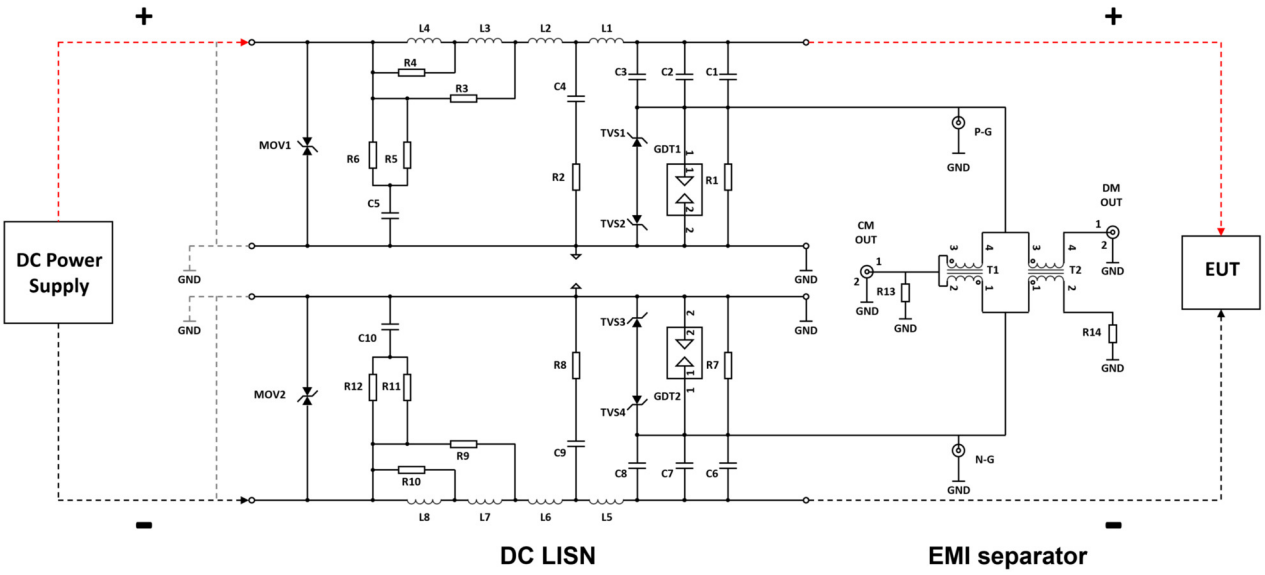

Fig. 2. Schematic design for the proposed DC LISN prototype.

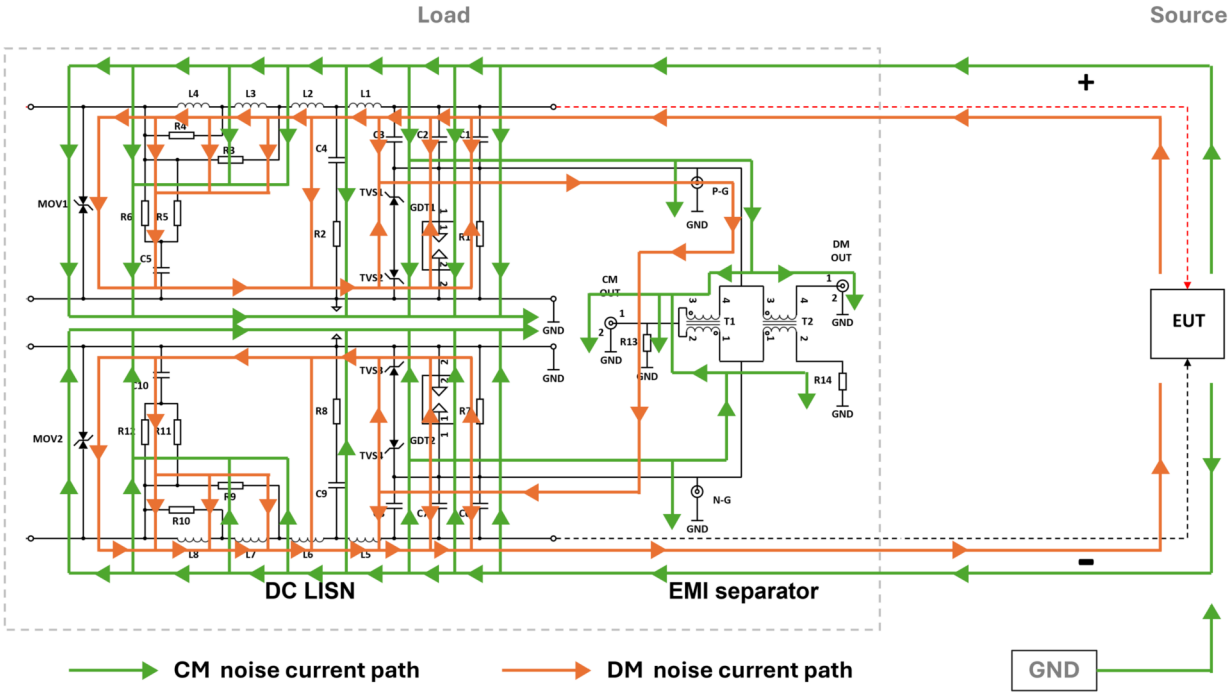

Fig. 3. CM and DM noise current paths for the proposed DC LISN prototype.

A. Schematic and Prototype of The Proposed Design

A schematic diagram of the proposed DC LISN is shown in Fig. 2. The design consists of a parallel configuration of a four-stage 5-µH topology [10, 18], an EMI separator circuit [14], and a protection circuit to ensure safe operation. To clarify the noise separation mechanism, the CM and DM current paths are illustrated in the equivalent circuit shown in Fig. 3. The prototype is shown in Fig. 4, with the main LISN components mounted on the top layer of the PCB and the EMI separator transformers (T1 and T2) mounted on the bottom layer to minimize the overall footprint. The PCB implementation presented in this work was developed primarily to realize and validate the proposed DC LISN architecture. Detailed optimization of PCB stack-up, grounding strategy, trace routing, and high-frequency parasitic-coupling effects was not investigated in this study.

B. Proposed DC LISN Components

The components used in the proposed DC LISN prototype are listed in Table I. According to CISPR 16-1-2, the components of a LISN must be selected to maintain an impedance of 50 Ω ± 20%, depending on the circuit topology and its intended application. In this paper, the design complies with

TABLE I
PROPOSED DC LISN COMPONENTS.

Part of Circuit	Component	Value	Type	Rated
DC LISN	R1, R7	1 kΩ	SMD	200 V
DC LISN	R2–R4, R8–R10	470 Ω	SMD	200 V
DC LISN	R5, R6, R11, R12	10 Ω	SMD	200 V
DC LISN	C1, C6	100 nF	SMD	250 V
DC LISN	C2, C7	1 nF	SMD	250 V
DC LISN	C3, C4, C8, C9	33 pF	SMD	500 V
DC LISN	C5, C10	220 nF	SMD	250 V
DC LISN	L1–L8	1.3 μH	SMD	16.5 A
Protection	GDT1, GDT2	5 mm	SMD	60 V
Protection	TVS1–TVS4	-	SMD	-
Protection	MOV1, MOV2	5 mm	SMD	270 V
EMI Separator	R13, R14	50 Ω	SMD	75 V
EMI Separator	T1, T2	780 μH	SMD	250 mA

CISPR 25 and adopts a 50 Ω/5 µH topology. As shown in Fig. 1, the circuit employs an RLC configuration with a 5-μH inductor to meet the requirements for EUT operation in low-voltage (LV) DC applications. The proposed DC LISN adopts a multistage configuration, with the number of stages selected to achieve optimal filtering performance. In this design, a four-stage configuration is employed, as proposed in [10]. The component list is provided below.

1) Resistors: Surface-mount device (SMD) resistors are selected for their low noise, suitability for high-frequency applications, and space efficiency on the PCB. Specifically, YAGEO (model RC1206FR-071KL) resistors are used for R1 and R7, TE Connectivity (model 3520470RJT) resistors for R2, R3, R4, R8, R9, and R10, and TE Connectivity (model 352010RJT) resistors for R5, R6, R11, and R12.

2) Capacitors: SMD ceramic capacitors are used in this circuit because of their compact size, high self-resonant frequency (SRF), wide availability, and suitability for the required electrical parameters. Specifically, YAGEO (model CC1206KRX7R9BB104) capacitors are used for C1 and C6, TDK (model C2012X7R2E102K085AA) capacitors for C2, and C7, Murata (model GRM21A5C2E330JW01D) capacitors for C3, C4, C8, and C9, and TDK (model C3225X7R2E224M200AE) capacitors for C5 and C10.

3) Inductors: The 5-μH inductance specified for the DC LISN is distributed across four stages, with each stage incorporating a 1.3-μH inductor. The four inductors are connected in series to achieve the required total inductance. Coilcraft (model MLC1250-132MLC) inductors are used for L1–L8 in the proposed design.

C. Additional Protection Circuit

This additional protection circuit is an enhancement designed for practical use, providing protection against transient overvoltage events. On the input side, metal oxide varistors (MOVs) are incorporated to suppress abnormal voltage spikes and help protect the DC LISN from transient disturbances. On the measurement side, gas discharge tubes (GDTs) and transient voltage suppression (TVS) diodes are employed to limit transient overvoltages and reduce the risk of damage to the EMI measurement circuitry. The selected GDT devices are specified by the manufacturer with a nominal spark-over voltage of 60 V and surge ratings of up to 20 kV and 2.5 kA under specified test conditions.

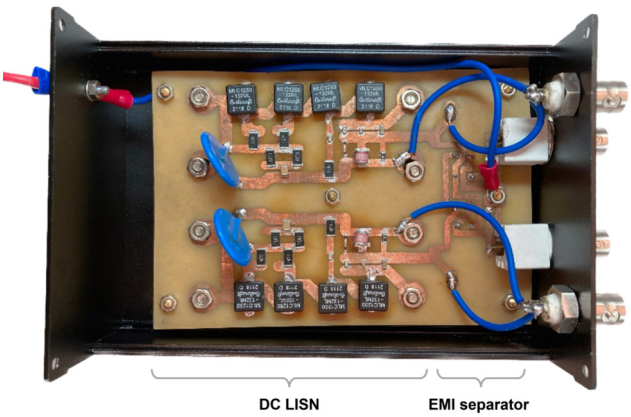

Fig. 4. The prototype implementation of the proposed DC LISN (Note: T1 and T2 are mounted on the bottom side of the PCB).

III. EMI SEPARATOR CIRCUIT

For conducted emission measurements, an EMI separator circuit is commonly used to separate EMI noise into differential-mode (DM) and common-mode (CM) components. The DM and CM noise voltages are derived from the sum and difference of the voltage vectors measured at the LISN output ports, namely, the positive-to-ground voltage (V_{PG}) and the negative-to-ground voltage (V_{NG}), across the 50-Ω terminations of the DC LISN. The DM and CM noise voltages are calculated using Eqs. (1) and (2), respectively.

$$|V_{\mathrm{DM}}| = |\frac{V_{PG} - V_{NG}}{2}|, \tag{1}$$

$$|V_{\mathrm{CM}}| = |\frac{V_{PG} + V_{NG}}{2}|. \tag{2}$$

According to [14], the schematic diagram of the EMI separator circuit is shown in Fig. 5. The output voltage at the positive-to-ground port (V_{PG}) of the DC LISN is assumed to be equal to the input voltage at the PG port (V_a) of the EMI separator circuit, while the output voltage at the negative-to-ground port (V_{NG}) is assumed to be equal to the input voltage at the NG port (V_b), as expressed in Eq. (3):

$$V_a = V_b = V_{PG}, \tag{3}$$

From Eqs. (2) and (3), the relationship can also be expressed in

terms of current, with R set to 50 Ω, leading to the expressions given in Eqs. (4) and (5).

$$I_a = I_b = \frac{V_{PG} - V_{NG}}{100}, \tag{4}$$

and for CM:

$$I_d = I_e = \frac{V_{PG} + V_{NG}}{100}, \tag{5}$$

Therefore, the input impedances can be determined by applying the current-divider principle to the currents at each port (I_1 and I_2), yielding an input impedance of 50 Ω per port. For the PG port, the input impedance is expressed in Eq. (6):

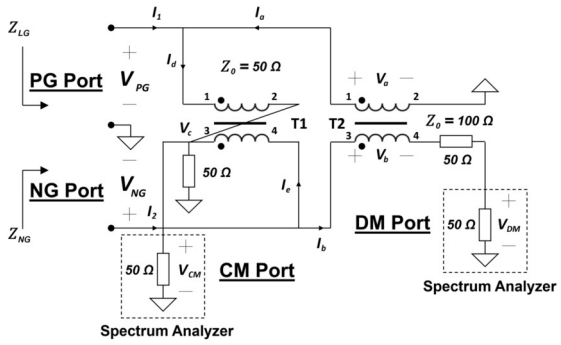

Fig. 5. Equivalent circuit proposed by S. Wong [14].

$$Z_{PG} = \frac{V_{PG}}{I_1} = \frac{V_{PG}}{I_d - I_a} = 50\Omega, \tag{6}$$

and for NG port, the input impedance is expressed in Eq. (7):

$$Z_{NG} = \frac{V_{NG}}{I_2} = \frac{V_{NG}}{I_b - I_e} = 50\Omega, \tag{7}$$

To achieve the calculated results, the transformer used for CM noise measurement must have an impedance of 50 Ω, whereas the transformer used for DM noise measurement must have an impedance of 100 Ω.

In the proposed EMI separator, all resistors are rated at 50 Ω, while transformers T1 and T2 (Coilcraft model WB1010-SMLD) have a characteristic impedance of 100 Ω and an inductance of 780 μH. To ensure accurate mode separation, the CM measurement path must present an impedance of 50 Ω. Following the methodology described in [14], the connection configuration of T1 is modified by joining pins 3 and 4, effectively adapting its nominal 100 Ω impedance to the required 50 Ω for CM noise measurement. This configuration ensures that the input impedance at both the P-G and N-G ports remains at 50 Ω, as confirmed by the derivations in Eqs. (6) and (7).

The integration of the EMI separator circuit does not compromise the fundamental performance of the DC LISN. According to the design principles described in [14], the separator maintains a purely resistive input impedance of 50 Ω, ensuring minimal insertion loss and compliance with standard measurement requirements. Furthermore, because the separator is connected downstream of the primary four-stage DC LISN, the isolation between the power input and the EUT output is preserved, as the separator does not interfere with the main filtering stages. Consequently, stable and reliable measurement conditions are maintained in accordance with CISPR 25.

IV. EXPERIMENTAL VALIDATION AND DISCUSSION

To evaluate the accuracy and effectiveness of the proposed DC LISN in maintaining a stable 50-Ω impedance and separating EMI noise, the experiments are divided into two main parts. First, the impedance at the output ports of the proposed DC LISN is simulated and compared with the measured results. Second, the noise separation performance is evaluated under two configurations: (1) the proposed DC LISN, comprising a four-stage DC LISN integrated with an EMI separator, and (2) a four-stage DC LISN without an EMI separator, used in conjunction with a current probe for EMI separation. The following sections describe the experimental procedures in detail.

A. DC LISN Circuit Model

As shown in Fig. 2, the impedance of the proposed DC LISN at the EUT-side ports, namely, the positive-to-ground and negative-to-ground ports, is derived in Eqs. (10) and (15), respectively.

Due to the symmetry of the proposed DC LISN, the impedance derivation is presented only for the positive branch. The negative branch can be derived in the same manner by replacing the corresponding component indices.

$$Z_C = \frac{1}{j\omega} \cdot \frac{\dfrac{1}{C_1C_2C_3}}{\dfrac{1}{C_1C_2} + \dfrac{1}{C_2C_3} + \dfrac{1}{C_1C_3}} \tag{8}$$

$$R_{\text{eq}} = \frac{R_1R_7}{R_1 + R_7} \tag{9}$$

$$Z_{\text{LISN}} = \frac{(Z + j\omega L_1)(Z_C + R_{\text{eq}})}{(Z + j\omega L_1) + (Z_C + R_{\text{eq}})} \tag{10}$$

where

$$Z_A = \frac{j\omega L_4 R_4}{j\omega L_4 + R_4} + j\omega L_3 \tag{11}$$

$$Z_B = \frac{R_5R_6}{R_5 + R_6} + \frac{1}{j\omega C_5} \tag{12}$$

$$Z_M = (Z_A \parallel R_3) + Z_B + j\omega L_2 \tag{13}$$

$$Z_N = R_2 + \frac{1}{j\omega C_4} \tag{14}$$

$$Z = \frac{Z_M Z_N}{Z_M + Z_N} \tag{15}$$

For simplicity, the equivalent impedances Z_A, Z_B, Z_M, Z_N, and Z are introduced to shorten the mathematical expressions

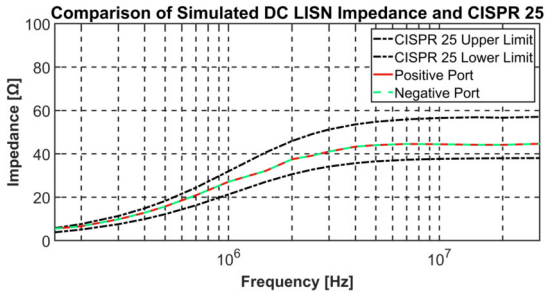

Fig. 6. Simulated impedance characteristics of the proposed DC LISN using PSpice.

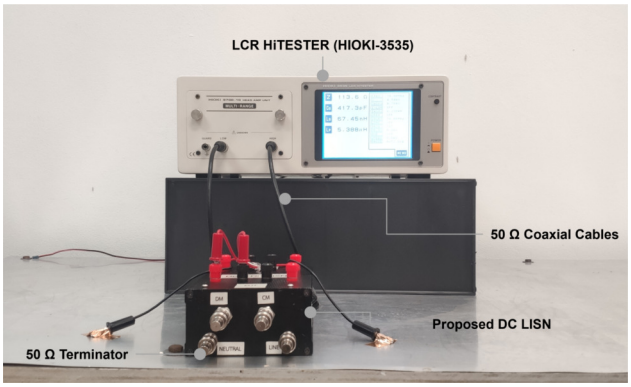

Fig. 7. Impedance measurement setup according to CISPR 16-1.

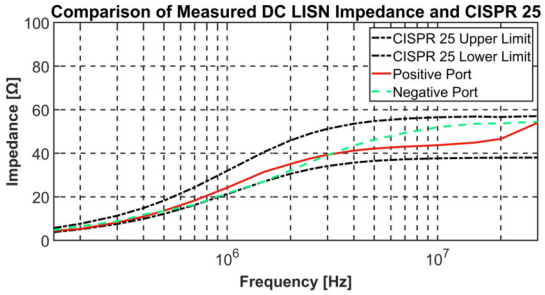

Fig. 8. Comparison of measured LISN impedance with CISPR 25 impedance limits.

and improve readability. The proposed DC LISN was simulated using PSpice to evaluate its impedance characteristics. An AC Sweep/Noise analysis was performed over a frequency range of 150 kHz to 30 MHz using a logarithmic frequency scale with 100 points per decade. The simulation results are compared with the impedance limits specified in CISPR 25, as shown in Fig. 6. The x-axis represents frequency over the range of 150 kHz to 30 MHz, while the y-axis represents impedance in ohms (Ω). The results verify the circuit's ability to maintain an impedance of 50 Ω within the specified tolerance. This simulation is an essential preliminary step in verifying the design before manufacturing the prototype. In deriving the LISN impedance (Z_{LISN}), the EMI separator circuit is modeled as a standard 50 Ω resistive termination. This assumption is supported by the design analysis presented in Section III, which demonstrates that the separator maintains a constant input impedance of 50 Ω over the measurement frequency range, as expressed in Eqs. (6) and (7). By adopting the parasitic-controlled design methodology described in [14], the separator effectively matches the input impedance of the spectrum analyzer, allowing the core RLC network of the LISN to be analyzed independently of the separator's internal complexity. Consequently, the analytical model in Eq. (10) remains practical and accurate for predicting LISN performance under standard operating conditions.

B. Experimental Testing of The DC LISN Prototype

Following the simulation, a prototype of the proposed DC LISN was fabricated, with the LISN circuitry and EMI separator integrated onto a single PCB. Experimental measurements were conducted to evaluate the output impedance in accordance with CISPR 16-1 requirements. To validate the design, the measured impedance was directly compared with the limits specified in CISPR 25. Rather than comparing the prototype with commercial LISNs, which are subject to the same ± 20% impedance tolerance, the impedance was measured directly using a calibrated LCR HiTESTER (HIOKI 3535). This approach provides a direct assessment of the prototype's impedance characteristics and verifies its compliance with the impedance requirements for automotive EMC testing.

The experimental setup is shown in Fig. 7. The measured impedance was compared with the CISPR 25 specification over the frequency range of 150 kHz to 30 MHz, as shown in Fig. 8. The results confirm that the impedance at both the positive and negative ports remains within the ±20% tolerance specified by CISPR 25 throughout the entire frequency range, validating the compliance and performance of the proposed prototype.

C. Conducted Emission Testing

Direct EMI measurements were performed at the output ports of the LISN. Fig. 9 shows the experimental setup for conducted EMI measurements. The setup consists of a 150 W DC–DC boost converter as the EUT, a 10 Ω resistive load, and the proposed DC LISN, all positioned on a reference ground plane in accordance with CISPR 25 requirements. The measured noise levels at the P–G and N–G ports are compared in Fig. 10. The results show nearly identical spectral profiles across the frequency range of 150 kHz to 30 MHz, confirming the symmetrical performance and design consistency of the proposed DC LISN prototype.

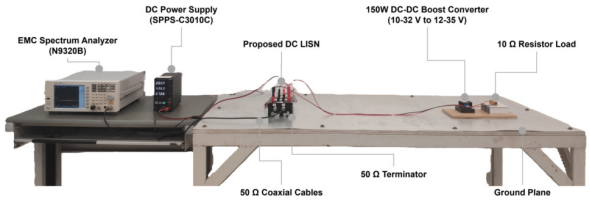

Fig. 9. Simulated impedance characteristics of the proposed DC LISN using PSpice.

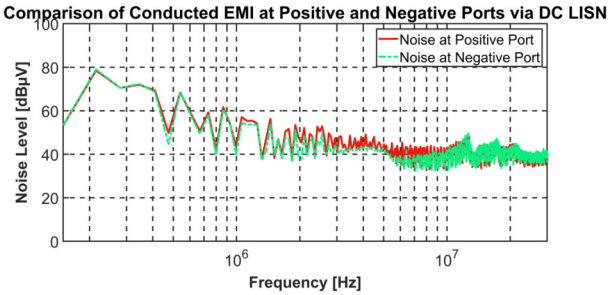

Fig. 10. Impedance measurement setup according to CISPR 16-1.

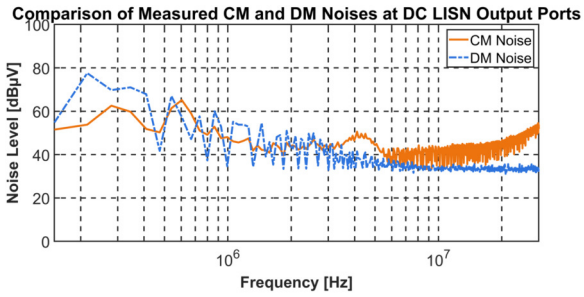

Fig. 11. Comparison of measured LISN impedance with CISPR 25 impedance limits.

Fig. 11 shows a clear distinction between the CM and DM spectra. In the frequency range from 150 kHz to 2 MHz, the DM levels were higher than the CM levels. Above 3 MHz, the CM amplitude gradually increased and eventually exceeded the DM level near 30 MHz. To validate the effectiveness of CM and DM separation, comparative measurements were performed using a calibrated current probe (model 111697), as shown in Fig. 12. These measurements provided an independent reference for verifying the spectral accuracy of the EMI separator. Additionally, to measure the DM current accurately using the current probe setup shown in Fig. 13, one of the two conductors must be reversed, typically by physically looping one wire in the opposite direction before clamping both conductors together. This technique, commonly used in EMI diagnostics, prevents the magnetic fields generated by the differential currents flowing in opposite directions from canceling each other, allowing the current probe to detect the net DM signal.

The CM and DM noise measurement results are shown in Fig. 14. Similar spectral patterns were observed, with DM noise dominating at lower frequencies and CM noise dominating above 3 MHz. These results demonstrate consistency between the LISN-based and current-probe-based measurements. The proposed EMI separator maintains effective DM and CM separation, and the LISN-based measurements exhibit spectral profiles similar to those obtained using the current probe.

The measurements were performed on a 1.0 mm-thick galvanized steel ground plane, which was electrically bonded to the surrounding environment to provide a stable reference. In accordance with CISPR 25 guidelines, the EUT and all interfacing cables were supported by non-conductive materials at a uniform height of 50 mm above the ground plane. Although the measurements were conducted outside a fully shielded chamber due to facility constraints, the primary objective was to validate the system's core capabilities, namely impedance stability and accurate noise mode separation. These conditions provide a practical assessment of the instrument's performance in diagnostic applications.

D. Validation Results and Analysis

The simulation and prototype measurement results indicate that the impedance at both the positive and negative ports remains within the 50 Ω ± 20% tolerance specified by CISPR 25 over the frequency range of 150 kHz to 30 MHz. As shown in Fig. 8, a slight discrepancy is observed between the measured impedances at the positive and negative ports. This difference is attributed to practical implementation constraints, including minor asymmetries in the PCB layout and manufacturing tolerances of the SMD components. Nevertheless, the impedance at both ports remains within the ± 20% tolerance specified by CISPR 25 across the entire frequency range, validating the robustness of the integrated prototype design. Furthermore, the integration of the EMI separator does not compromise compliance with the standard, confirming the effectiveness of the proposed design.

Regarding EMI separation, the CM noise measurements obtained using the proposed DC LISN agree well with those obtained using a current probe, as shown in Fig. 11 and Fig. 14. However, CM noise attenuation is observed in the lower frequency range of 150 kHz to 2 MHz. Similar behavior is also observed in the current-probe measurements. The observed trend is therefore considered to originate from the EMI characteristics of the EUT rather than from limitations of the proposed EMI separator. To evaluate the spectral characteristics and effectiveness of the integrated EMI separator, a calibrated current probe was used as an independent reference to verify the identification of dominant CM and DM noise components. The comparison was intended to assess consistency in spectral characteristics and noise-mode separation. A quantitative uncertainty analysis and point-by-point error comparison were not performed in this study and are considered future work. The strong agreement in spectral profiles and mode dominance between the proposed DC LISN and the current probe measurements, as shown in Fig. 11 and Fig. 14, demonstrates that the instrument can reliably identify dominant CM and DM noise components and reproduce the corresponding spectral characteristics. This comparative validation suggests that the integrated separator preserves the overall spectral characteristics while offering the practical advantage of simultaneous CM and DM separation. In addition, a slight discrepancy is observed at frequencies above 20 MHz, where the separated-mode levels in Fig. 11 are marginally higher than the total noise levels in Fig. 10. This behavior is attributed to parasitic effects in the integrated EMI separator. Consistent with the findings reported in [14], high-frequency parasitic resonances, particularly those associated with transformer winding capacitances and PCB trace impedances, can degrade separator performance and cause deviations in the input impedance.

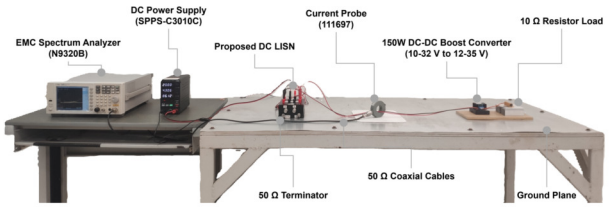

Fig. 12. Experimental setup for conducted EMI measurement by using the current probe.

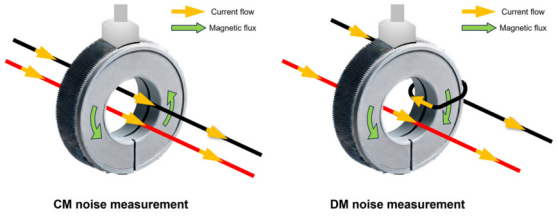

Fig. 13. Separation of CM and DM currents by using current probes.

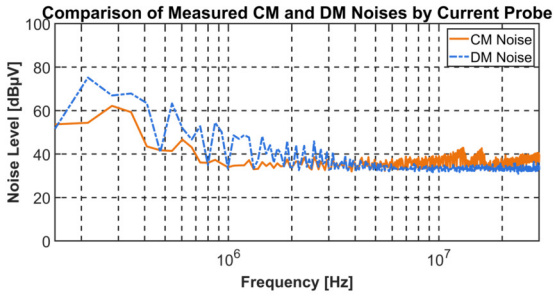

Fig. 14. Comparison of measured CM and DM noises by using the current probe.

Overall, the comparative analysis confirms that the proposed DC LISN maintains a stable 50 Ω impedance while effectively separating CM and DM noise components. Despite minor deviations at higher frequencies, the comparison with current-probe measurements supports its suitability for EMI diagnostics and pre-compliance conducted-emission evaluation.

V. Conclusion

This paper has presented the design and validation of a DC LISN that maintains impedance within the limits specified by CISPR 25 while integrating an EMI separator for simultaneous CM and DM measurements. Experimental results demonstrate that the proposed DC LISN provides a practical platform for conducted EMI diagnosis and pre-compliance evaluation, while maintaining impedance characteristics consistent with CISPR 25 requirements. The measurements were conducted to validate the functionality of the proposed DC LISN and EMI separator under practical laboratory conditions. Its ability to measure EMI noise from both the positive and negative lines within a single circuit eliminates the need for multiple LISNs and external separators, thereby improving measurement efficiency and practicality. Furthermore, the proposed design provides a compact and lower-cost alternative to commercially available solutions while offering integrated CM and DM noise separation capability.

Despite these advantages, certain limitations remain, particularly in the absolute amplitude accuracy of the separated noise levels under some frequency conditions. These limitations are attributed to parasitic impedance effects and the limited variety of DC loads evaluated in the experimental setup. Future work will focus on mitigating parasitic effects and extending validation to a broader range of load conditions to improve measurement accuracy and generalizability. Furthermore, validation in a fully compliant shielded chamber is planned to improve measurement accuracy and ensure consistency with standardized testing environments. Overall, the proposed DC LISN addresses key limitations of conventional designs and provides a practical, compact, and cost-effective solution for conducted EMI measurements and diagnostics in DC applications. With further refinement, it could form part of pre-compliance testing infrastructure for academic and industrial research on low-voltage DC equipment.

VI. Acknowledgement

The authors would like to thank Mr. Jaknarin Sukkai, Mr. Shitipat Thongdee, Mr. Sermsak Sripradab, and Mr. Chanon Akaphobanukul for their valuable contributions to the experimental demonstrations.

References

[1] G. Arunkumar, D. Elangovan, P. Sanjeevikumar, J. B. H. Nielsen, Z. Leonowicz, and P. K. Joseph, “DC grid for domestic electrification,” *Energies*, vol. 12, Art. no. 2157, 2019.

[2] L. T. Berger, A. Schwager, and J. J. Escudero-Garzás, “Power line communications for smart grid applications,” *J. Electr. Comput. Eng.*, vol. 2013, Art. no. 712376, 2013.

[3] D. Kumar, F. Zare, and A. Ghosh, “DC microgrid technology: System architectures, AC grid interfaces, grounding schemes, power quality, communication networks, applications, and standardizations aspects,” *IEEE Access*, vol. 5, pp. 12230–12256, 2017.

[4] D. Wang, D. Weyen, and P. Van Tichelen, “Proposals for updated EMC standards and requirements (9–500 kHz) for DC microgrids and new compliance verification methods,” *Electronics*, vol. 12, no. 14, Art. no. 3122, 2023.

[5] A. E. Shadare, M. N. O. Sadiku, and S. M. Musa, “Electromagnetic compatibility issues in critical smart grid infrastructure,” *IEEE Electromagn. Compat. Mag.*, vol. 6, no. 4, pp. 63–70, 2017.

[6] Y. Zhao, K. Y. See, S. J. Li, N. Q. Jiang, Q. Wang, Y. Cao, and X. H. Wu, “Current probe method applied in conductive electromagnetic compatibility (EMC),” in *Proc. Int. Conf. Microw. Millim. Wave Technol. (ICMMT)*, 2008, vol. 3, pp. 1442–1445.

[7] C. R. Paul and K. B. Hardin, “Diagnosis and reduction of conducted noise emissions,” *IEEE Trans. Electromagn. Compat.*, vol. 30, no. 4, pp. 553–560, 1988.

[8] D. Sakulhirirak, V. Tarateeraseth, W. Khan-ngern, and N. Yoothanom, "Design of high performance and low cost line impedance stabilization network for university power electronics and EMC laboratories," in *Proc. 7th Int. Conf. Power Electron. Drive Syst. (PEDS)*, 2007, pp. 284–289.

[9] I. Grobler and M. N. Gitau, "Low cost power lead extended pre-compliance conducted EMI measurement setup and diagnostics with compact LISN," in *Proc. IEEE ECCE Asia Downunder*, 2013, pp. 1144–1149.

[10] R. Amjadifard, M. Tavakoli Bina, H. Khaloozadeh, and F. Bagheroskouei, "Proposing an improved DC LISN for measuring conducted EMI noise," *IEEE Trans. Electromagn. Compat.*, vol. 63, no. 3, pp. 752–761, 2021.

[11] T. Guo, D. Y. Chen, and F. C. Lee, "Separation of the common-mode- and differential-mode-conducted EMI noise," *IEEE Trans. Power Electron.*, vol. 11, no. 3, pp. 480–488, 1996.

[12] A. Nagel and R. W. De Doncker, "Separating common mode and differential mode noise in EMI measurement," *EPE J.*, vol. 10, no. 2, pp. 27–30, 2000.

[13] M. C. Caponet and F. Profumo, "Devices for the separation of the common and differential mode noise: Design and realization," in *Proc. 17th Annu. IEEE Appl. Power Electron. Conf. Expo. (APEC)*, 2002, vol. 1, pp. 100–105.

[14] S. Wang, F. C. Lee, and W. G. Odendaal, "Characterization, evaluation, and design of noise separator for conducted EMI noise diagnosis," *IEEE Trans. Power Electron.*, vol. 20, no. 4, pp. 974–982, 2005.

[15] S. Schroth, F. Krismer, J. W. Kolar, and H. Ertl, "Analysis and practical relevance of CM/DM EMI noise separator characteristics," in *Proc. 16th Eur. Conf. Power Electron. Appl. (EPE)*, 2014, pp. 1–10.

[16] D. Sakulhirirak, V. Tarateeraseth, W. Khan-ngern, and N. Yoothanom, "A new simultaneous conducted electromagnetic interference measuring and testing device," in *Proc. Asia-Pacific Symp. Electromagn. Compat. and 19th Int. Zurich Symp. Electromagn. Compat.*, 2008, pp. 606–609.

[17] J. Stahl, D. Kuebrich, and T. Duerbaum, "Modification and characterization of a standard LISN for effective EMI noise separation," in *Proc. Int. Conf. Electromagn. Adv. Appl. (ICEAA)*, 2010, pp. 39–42.

[18] TekBox Digital Solutions, "TBOH01 5 μH line impedance stabilisation network (LISN)—CISPR 25." [Online]. Available: https://www.tekbox.com/product/tboh01-5uh-lisn-cispr-25/



Warathep Padungtin received the B. Eng. and M. Eng. Degree in electrical engineering from Srinakharinwirot University, Thailand. Currently, he has been an EMC Engineer with the Turnkey & Infrastructure department, ALSTOM Transport Systems. His research interests are mainly in the fields of Power Electronics and Electromagnetic Compatibility.



Vuttipon Tarateeraseth received both the B. Eng. (second-class honors) and M. Eng. Degree in electrical engineering from King's Mongkut Institute of Technology Ladkrabang (KMITL), Thailand, and Ph.D. in Electronics and Communications Engineering from Polytechnic University of Turin, Italy. He was a visiting researcher at the Nanyang Technological University, Singapore, from July 2008 to July 2009. Currently, he has been an Associate Professor in the Department of Electrical Engineering at the Srinakharinwirot University, Thailand. His research interests are mainly in the fields of Power Electronics and Electromagnetic Compatibility.